

A Comprehensive Evaluation on Quantization Techniques for Large Language Models

Yutong Liu^a, Cairong Zhao^{a,*}, Guosheng Hu^b

^a*Department of Computer Science and Technology, Tongji University, Shanghai 201804, China*

^b*School of Engineering Math and Technology, University of Bristol, BS8 1QU, UK*

Abstract

For large language models (LLMs), post-training quantization (PTQ) can significantly reduce memory footprint and computational overhead. Model quantization is a rapidly evolving research field. Though many papers have reported breakthrough performance, they may not conduct experiments on the same ground since one quantization method solution usually contains multiple components. In addition, it is also important to analyze the theoretical connections among numerous existing methods to gain in-depth understanding in this field. To bridge these gaps, in this paper, we timely conduct an extensive review of the state-of-the-art methods and also perform comprehensive evaluations on the same ground to ensure fair comparisons of these methods. To our knowledge, this fair and extensive investigation remains critically important yet significantly underexplored in the research community.

To better understand the theoretical connections, we decouple the published quantization methods into two steps: pre-quantization transformation and quantization error mitigation. We define the former as a preprocessing step applied before quantization to reduce the impact of outliers, making the data distribution flatter and more suitable for quantization. Quantization error mitigation, on the other hand, involves techniques that offset the errors introduced during quantization, thereby enhancing model performance. Meanwhile, we extensively evaluate and analyze the impact of different components of quantization methods. Additionally, we also timely analyze and

*Corresponding author.

Contact: 2432031@tongji.edu.cn, zhaocairong@tongji.edu.cn, g.hu@bristol.ac.uk.

evaluate the latest MXFP4 data format and its performance. Our experimental results demonstrate that the optimized rotation and scaling yield the best performance for pre-quantization transformation, and combining low-rank compensation with GPTQ occasionally outperforms using GPTQ alone for quantization error mitigation. Furthermore, we explore the potential of the latest MXFP4 quantization and reveal that the optimal pre-quantization transformation strategy for INT4 does not generalize well to MXFP4, inspiring further investigation in this field.

Keywords: Model Quantization, Post-training Quantization, LLM

1. Introduction

Large language models (LLMs) have achieved remarkable performance on diverse tasks and are increasingly being applied in various scenarios. Nonetheless, LLMs inference process incurs significant memory and computational overhead, leading to high inference latency and posing challenges for computations on source-limited GPUs.

Post-training quantization (PTQ) is a promising solution to reduce the memory and computational cost of LLMs, enhancing their inference efficiency. LLMs quantization has been studied in a wide spectrum of precision configurations. Representative settings include W4A4 [1, 2, 3, 4], W8A8 [5, 6, 7] and W4A16 [8, 9, 10, 11]: W4A4 quantizes both weights and activations to 4-bit precision (INT4); W8A8 and W4A16 quantize weights to INT8 and INT4 and activations to INT8 and FP16/BF16 respectively. Among these 3 settings, W4A4 is the current research focus because it provides the best performance in terms of both memory efficiency and inference speed, with the greatest research significance.

However, despite the wide range of methods explored in previous studies, W4A4 quantization still struggles to achieve lossless performance, especially for smaller LLMs, such as those with 1B, 3B, and 7B parameters, which often results in increased perplexity and degraded performance on various tasks. Furthermore, LLaMA3 experiences a larger performance drop after quantization compared to LLaMA2 when using many popular quantization methods [3, 4, 12], facing a greater demand for better W4A4 quantization methods. Therefore, W4A4 quantization for LLMs still remains a challenging task.

To review and evaluate the state-of-the-art quantization methods, in particular, under the setting of W4A4, we find two main characteristics of these methods. First, existing methods are often combinations of multiple techniques, since using a single technique alone typically fails to achieve excellent quantization performance. In SpinQuant [3], after applying trained rotations to adjust the model, the GPTQ [8], a gradient-based quantization error mitigation method is further applied to quantize the rotated weights. Similarly, OSTQuant [8] employs multiple techniques to adjust the weights and activations, including rotation and scaling. At the same time, there are many weight-only quantization methods, some of which can be combined with pre-quantization transformation techniques and extended to weight-activation quantization. AWQ [11] shares similar pre-quantization transformation (scaling) with SmoothQuant [6], even though their motivations differ. Also, QuIP# [10] shares similar pre-quantization transformation (random hadamard rotation) with QuaRot [13]. Apart from the methods that involve both weight and activation transformations, there are also approaches that are orthogonal to pre-quantization transformation that can be used to compensate for the loss between quantized models and full precision models, such as GPTQ [8] and low-rank branches computed from quantization error [14, 15, 16]. Second, quantization involves a variety of configurations, such as granularity and symmetric or not. Different settings can lead to different performance outcomes and often involve trade-offs between efficiency and accuracy. For different precision levels, the optimal quantization settings may vary. Evaluating the performance under various quantization configurations for W4A4 quantization is of great importance.

In this paper, as aforementioned in the first characteristic, the existing quantization solutions are very complicated and they usually consists of many algorithms. To make our evaluation on the same ground and achieve a better understanding of existing methods, we decompose the quantization process into two key steps: pre-quantization transformation and quantization error mitigation. The pre-quantization transformation step refers to preprocessing the data before quantization in order to mitigate the effect of outliers making the data distribution smoother and more quantization-friendly. The quantization error mitigation step involves applying techniques to compensate for the errors introduced by quantization, thereby reducing the overall quantization error and improving performance. For each step, we select several state-of-the-art techniques and conduct an evaluation of the effectiveness of their combinations. Second, existing solutions usually do not use exactly

the same setting, e.g. granularity, leading to unfair comparison. To bridge this gap, we conduct a comprehensive evaluation on the same quantization configurations and provide recommendations on selecting appropriate configurations. And we integrate the methods used in this paper in our code library to facilitate performance evaluation.

Furthermore, the NVIDIA’s GeForce RTX 50 Series latesty released based on the new RTX Blackwell architecture includes support for the FP4 data format, including NVFP4 and MXFP4, in its new Tensor Cores, which show great advantages over INT4. However, the research on FP4 has not been well explored. To bridge this gap, we conduct research on weight-activation FP4 quantization using the popular methods in INT4, showing the great timeliness of our research.

Methods	Data Normalization	Error Compensation
SmoothQuant [6]	scale	-
Outlier Suppression+ [7]	scaling + shifting	-
GPTQ [8]	-	GPTQ
ZeroQuant-v2 [14]	-	low-rank
QuIP [9]	rotation	GPTQ
AWQ [11]	scaling	-
Atom [1]	reorder	GPTQ
OmniQuant [2]	optimized scaling + shifting	GPTQ
Qserve [17]	scaling + rotation	GPTQ
LQER [18]	-	low-rank
QuaRot [13]	rotation	GPTQ
SpinQuant [3]	optimized rotation	GPTQ
ResQ [19]	reorder + rotation	GPTQ
FlatQuant [12]	optimized scaling + rotation	GPTQ
OSTQuant [4]	optimized scaling + rotation	GPTQ

Table 1: Two steps decomposition of quantization methods.

2. Review on Existing Quantization Methods

In this section, we first review recent quantization algorithms in Section 2.1 and Section 2.2 in terms of two steps: pre-quantization transformation and quantization error mitigation. Table 1 shows our decomposition of the popular quantization methods. Section 2.3 and Section 2.4 focus on settings,

including symmetricity and granularity of quantization methods. Meanwhile, Table 2 summarizes the quantization settings reported in the experimental results of these methods.

Methods	Precision	Symmetric		Granularity
		W	A	
SmoothQuant [6]	W8A8	T	F	T,C
GPTQ [8]	W3A16,W4A16	T	-	G
ZeroQuant-v2 [14]	W4A16,W3A16,W2A16,W4A8	T,F	T,F	G
QuIP [9]	W2A16,W3A16,W4A16	T	-	G
AWQ [11]	W3A16,W4A16	T	-	G
Atom [1]	W3A3,W4A4	T	F	G
OmniQuant [2]	W2A16,W3A16,W4A16,W4A4,W6A6,W8A8	F	F	C
Qserve [17]	W4A8	T	F	C
LQER [18]	W4A6,W4A8	T	F	G
QuaRot [13]	W4A4	T	F	C,G
SpinQuant [3]	W4A4,W4A8	T	F	C
ResQ [19]	W4A4	T	F	C
FlatQuant [12]	W4A4	T	F	C
OSTQuant [4]	W4A4	T	F	C

Table 2: Symmetry and granularity of quantization methods. In granularity, T stands for per-tensor, C represents per-channel or per-token, and G means per-group

2.1. Pre-quantization transformation

Pre-quantization transformation is a step before quantization, applying operations such as shifting, scaling, and rotation to process weights and activations. These transformations aim to flatten and smooth the hard-to-quantize tensors, thereby enhancing the quantization performance. LLMs are difficult to quantize due to the outliers in the activations. Compared to most of the activation values, the magnitude of outliers is substantially higher, often exceeding 100x larger in some layers. The outliers will dominate the maximum magnitude measurement, leading to low effective quantization levels. This pre-quantization transformation step is illustrated in Fig. 1.

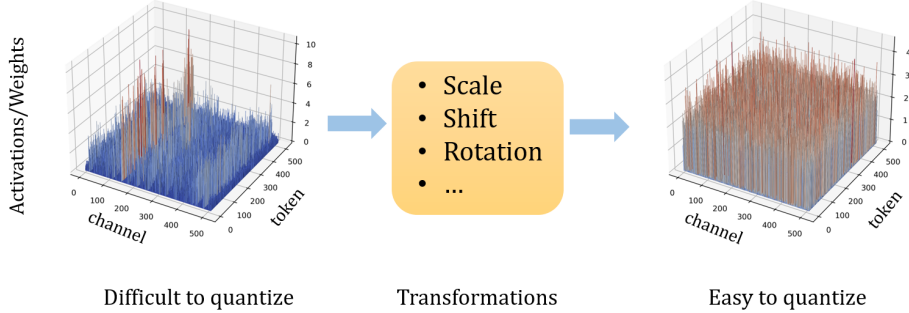


Figure 1: Pre-quantization transformation: Transforming activations and weights to render them more easier to quant

2.1.1. Shifting

Activations distribution is often asymmetric, and this asymmetry varies across different channels. Aligning the center of each channel can improve the performance of quantization, since we quantize activations per-token rather than along the channel dimension. Outlier Suppression+ [7] proposes shifting activation values to eliminate the asymmetry feature across channels. The shifting process is to use a vector that transfer the channels of the activation. For a linear layer, it is formulated as:

$$Y = XW + B = \underbrace{((X - T))}_{\hat{X}}W + \underbrace{(TW + B)}_{\hat{B}} \quad (1)$$

where the layer input $X \in \mathbb{R}^{T \times C_{in}}$ is shifting and becomes \hat{X} . $T \in \mathbb{R}^{1 \times C_{in}}$ is a vector representing the channel-wise shifting parameters. To keep mathematical equivalent, an additional term, the product of T and $W \in \mathbb{R}^{C_{in} \times C_{out}}$, is added to the bias $B \in \mathbb{R}^{1 \times C_{out}}$. Outlier Suppression+ [7] uses calibration to get the vector T , which is computed channel-wise as the average of its minimum and maximum values:

$$t_i = \frac{\min(X_i) + \max(X_i)}{2} \quad (2)$$

where t_j denotes the j -th element of T , corresponding to the j -th channel. X_j represents the j -th input channel of X . OmniQuant [2] employs learnable channel-wise shifting for outlier suppression, combined with the learnable scaling technique discussed in Section 2.1.2, and jointly optimize these two kinds of pre-quantization transformation parameters.

2.1.2. Scaling

Scaling is a commonly used pre-quantization transformation method, which scales activations in different input channels before quantization, and inversely scales the corresponding weight channels to make the results stay unchanged. SmoothQuant [6] first propose using scaling to smooth the quantization difficulty from activations to weights. Compared to weights, activations have more outliers that make quantization harder. It is observed that outliers in activations appear in certain channels, so applying channel-wise scaling to activations can eliminate the outliers to a certain degree, using the following equation for linear layers:

$$Y = XW = \underbrace{(X \cdot S^{-1})}_{\hat{X}} \underbrace{(S \cdot W)}_{\hat{W}} = \hat{X}\hat{W} \quad (3)$$

where the weights of a linear layer W and the layer input X is scaling and becomes \hat{X} and \hat{W} . S is a diagonal matrix composed by scaling factors of different channels, which can be obtained in various ways. SmoothQuant [6] uses calibration to compute S . The calibration process can be formulated as:

$$s_j = \max(|X_j|)^\alpha / \max(|W_j|)^{1-\alpha} \quad (4)$$

where X_j and W_j denote the j -th input channel of X and W , respectively. s_j is the j -th diagonal element of S , corresponding to the j -th channel. α is a hyperparameter that controls the degree to which outliers are transferred between activations and weights.

AWQ [11], as a weight-only quantization method, approaches the problem from the perspective of protecting salient weights, applying activation-aware scaling. Unlike adopting the hand-crafting parameters in calibration, the scaling operation in OmniQuant [2] uses learnable scaling, where S is learnable parameters that are optimized with block-wise quantization error minimization.

FlatQuant [12] and OSTQuant [4] both use learnable per-channel scaling, but at different stages of pre-quantization transformation, leading to different practical meanings. Both perform a diagonal scaling operation, yet FlatQuant scales before rotation, allowing its scaling factors to be initialized via Eq. (4), functionally similar to SmoothQuant. In contrast, OSTQuant applies scaling after rotation, meaning this diagonal scaling is a post-rotation adjustment rather than smoothing the original channels.

2.1.3. Rotation

The rotation operation is a technique that adjusts data distribution by multiplying the data matrix with an orthogonal matrix. This operation largely changes the activation distributions, reduces outliers in the data and thereby enhancing quantization accuracy. The rotation process in a linear layer can be formulated as:

$$Y = XW = \underbrace{(XO)}_{\hat{X}} \underbrace{(O^T W)}_{\hat{W}} = \hat{X}\hat{W} \quad (5)$$

where the input X is rotated with an orthogonal matrix O , resulting in $\hat{X} = XO$. To preserve the model’s output, the weight W is simultaneously transformed by O^T , which is the transpose of O .

QuIP [9] first introduced rotation with random orthogonal matrices to reduce incoherence in weight-only quantization. QuIP# [10] replaces this with random Hadamard matrices for greater efficiency. QuaRot [13] extends rotation to both weights and activations quantization using random Hadamard matrices, effectively eliminating outliers. SpinQuant [3] further improves stability by optimizing the rotation matrix on the Stiefel manifold to minimize quantization-induced performance variance, while still defaulting to random Hadamard for a few online rotations.

Rotation is a highly effective pre-quantization transformation technique for reducing outliers in low-bit quantization, and it has also been widely adopted in many other quantization methods (*e.g.*, ResQ [19], QServe [17], FlatQuant [12] and OSTQuant [4], etc), which combine rotation with other pre-quantization transformation techniques to further improve performance.

2.2. Quantization error mitigation

The quantization error mitigation step employs techniques that mitigate the error introduced by quantization by compensating them. This error between the original model and the quantized model can be computed from calibration datasets, and be compensated to the original weights in linear layers or through low-rank branches. Fig. 2 demonstrates two commonly used quantization error mitigation methods.

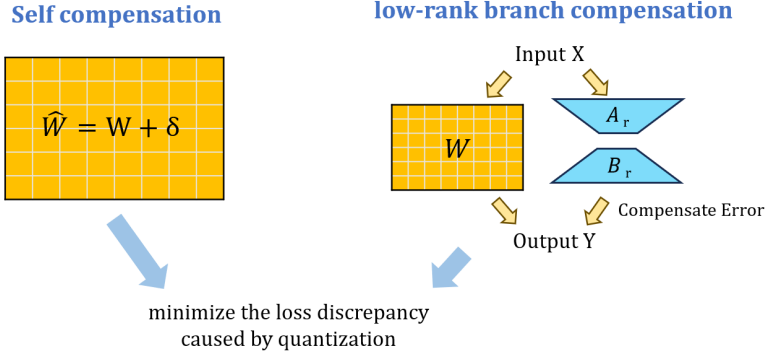


Figure 2: Quantization error mitigation: compensate the error produced by quantization. (1) Self-compensation [8, 9] calculates weight compensation terms through quantization-induced loss errors; (2) Low-rank branch compensation [14, 16, 18, 15] constructs auxiliary compensation pathways via matrix factorization of post-quantization weight errors.

2.2.1. Self compensation

GPTQ [8] is a quantization method for weight quantization that uses Hessian-based quantization error mitigation. GPTQ builds on the OBQ [20] method that solves the error introduced by quantization and the optimal weight perturbation. For weight quantization, the loss error introduced by quantization can be defined as:

$$\epsilon = \mathcal{L}(W_q) - \mathcal{L}(W) = \mathcal{L}(W + \delta) - \mathcal{L}(W) \quad (6)$$

where $L(W)$ is the loss function of the model evaluated at weights W , and δ represents the weight perturbation. Using a Taylor expansion, we can get the Hessian-based approximation of the quantization loss, which can be formulated as:

$$\epsilon = \nabla \mathcal{L}(W)^\top \delta + \frac{1}{2} \delta^\top H(W) \delta + \mathcal{O}(\|\delta\|^3) \approx \frac{1}{2} \delta^\top H(W) \delta \quad (7)$$

Unlike OBQ that uses greedy order to quantize weights, GPTQ quantized all rows of weights in a fixed order. The GPTQ algorithm performs quantization column by column in blocks of size B . For each column within the block, the quantization error is computed when quantized, and then compensates on the remaining weights. Once all columns of a block is quantized, the remaining weights in the matrix are also updated.

QuIP [9] also minimizes a quadratic proxy of the weight error to implement an optimal adaptive rounding procedure called LDLQ. In this method, an LDL decomposition of the Hessian matrix is performed to construct a feedback matrix U , which is then used to form a compensation term that corrects for the quantization-induced error. In QuIP, it is proven that for Eq. (7), performing an LDL decomposition on the Hessian matrix yields an optimal choice of U , and GPTQ is a special case of LDLQ.

2.2.2. Low-rank branch compensation

Beyond compensating errors directly on the original weights, an alternative approach is to introduce an auxiliary branch dedicated to error correction. Some prior works leverage a low-rank term to reconstruct quantization error (*e.g.*, ZeroQuant-v2 [14], CALDERA [16], LQER [18], QERA [15], etc). After incorporating a low-rank branch, the output Y is computed as:

$$Y = XW = XW_q + X\Delta W \approx XW_q + XAB \quad (8)$$

where $\Delta W = W - W_q$ denotes the weight reconstruction error introduced by quantization. $A \in \mathbb{R}^{C_{in} \times r}$, $B \in \mathbb{R}^{r \times C_{out}}$ are learnable low-rank matrices, and $r \ll \min(d, k)$ is the bottleneck rank. The product $AB \in \mathbb{R}^{d \times k}$ serves as a low-rank approximation of the quantization error.

ZeroQuant-v2 [14] and LQER [18] reconstruct the weight quantization error through SVD-based low rank approximation. LQER computes the low rank matrices A, B by using SVD composition to the quantization error matrix ΔW :

$$\Delta W = U\Sigma V^T \approx \underbrace{U_k}_{A_k} \cdot \underbrace{\Sigma_k V_k^T}_{B_k} = A_k B_k \quad (9)$$

where $U \in \mathbb{R}^{m \times n}$, $V \in \mathbb{R}^{n \times n}$, $\Sigma \in \mathbb{R}^{m \times n}$ and $U_k \in \mathbb{R}^{m \times k}$, $V_k \in \mathbb{R}^{n \times k}$, $\Sigma_k \in \mathbb{R}^{k \times k}$.

Based on LQER, L²QER, which is proposed in LQER, scales the ΔW before applying SVD, and inversely apply scales in A_k . This operation aims to more precisely approximated the quantization error corresponding to the salient weights. The process can be formulated as:

$$\Delta \hat{W} = S\Delta W = U\Sigma V^T \approx \underbrace{U_k}_{A_k} \cdot \underbrace{\Sigma_k V_k^T}_{B_k} = A_k B_k \quad (10)$$

$$\hat{A}_k = S^{-1}A_k, \hat{B}_k = B_k \quad (11)$$

In addition to the aforementioned approaches, CALDERA [16] and QERA [15] provide analyses from different perspectives, deriving the optimal low-rank terms for quantization error reconstruction. In contrast to approaches that introduce low-rank branches externally, QwT [21] integrates lightweight linear layers within each decoder layer block of LLMs, directly compensate quantization errors, offering new insights for quantization error mitigation.

2.3. Symmetric vs. asymmetric

Uniform quantizers can be broadly categorized into **symmetric** and **asymmetric** schemes, depending on how the zero point is handled during the mapping from floating-point to integer values.

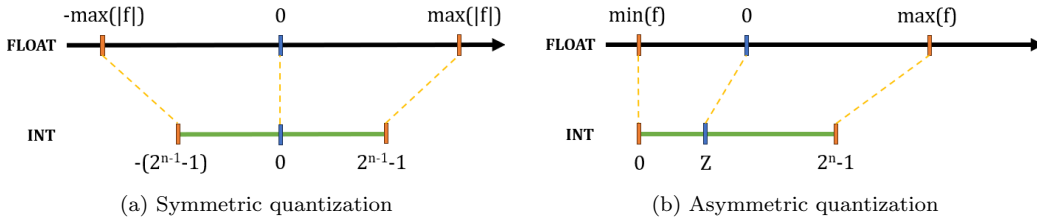


Figure 3: Symmetry of quantization

Symmetric quantization forces the zero point to align with the floating point, resulting in a quantization range that is symmetric with respect to zero. The quantization process is typically defined as:

$$X_q = \text{round} \left(\frac{X}{\Delta} \right), \quad \Delta = \frac{\max(|X|)}{2^N - 1} \quad (12)$$

where the floating-point tensor X is scaled by a parameter Δ , which is computed from the distribution of X . Eq. (12) presents a commonly used Min-Max method for computing the quantization step size Δ , where N denotes the bit-width of the quantization precision.

The dequantization process can be formulated as:

$$\text{dequant}(X) = X_q \Delta \quad (13)$$

$$\text{dequant}(Y_q) = X_q W_q \Delta_X \Delta_W = Y_q \Delta_X \Delta_W \quad (14)$$

It is evident that symmetric quantization enables a very simple dequantization process. For linear layers, dequantization can be efficiently performed

by multiplying the quantized output with the product of the scale factors for the weights and activations like Eq. (14). This simplifies computation and is often preferred in hardware implementations. However, symmetric quantization may lead to suboptimal representation when the data distribution is not centered around zero.

Asymmetric quantization allows the zero point to shift dynamically according to the minimum and maximum values of the data. This enables a tighter fit to the data distribution, especially when it is skewed, at the cost of slightly more complex computation.

Asymmetric quantization incurs additional computational cost during dequantization, while it often outperforms symmetric quantization in terms of accuracy. The dequantization process can be formulated as:

$$\text{dequant}(X) = (X_q - Z)\Delta \tag{15}$$

$$\begin{aligned} \text{dequant}(Y_q) &= (X_q - Z_X)\Delta_X \cdot (W_q - Z_W)\Delta_W \\ &= Y_q\Delta_X\Delta_W + (Z_XW_q + Z_WX_q + Z_XZ_W)\Delta_X\Delta_W \end{aligned} \tag{16}$$

As such, the selection of quantization symmetry should be made with consideration of the specific use case and performance-complexity trade-offs.

2.4. Granularity of quantization

The granularity of quantization often largely effects the low-bit quantization performance. Commonly adopted granularities include per-tensor, per-channel or per-token, and per-group, as illustrated in Fig. 4.

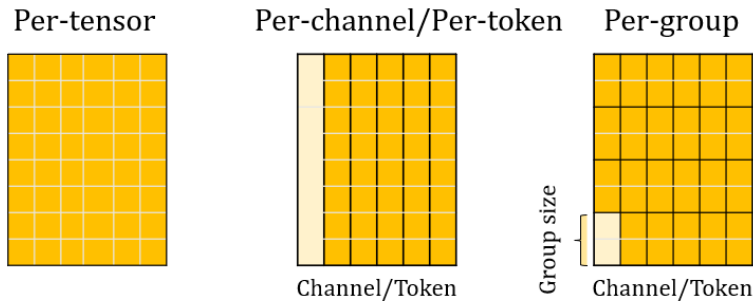


Figure 4: Granularity of quantization: (1) Per-tensor quantization; (2) Per-channel quantization; (3) Per-group quantization.

In per-tensor quantization, a single set of affine transformation parameters is applied to the entire tensor, with the scale (Δ) and zero point (Z) computed from the tensor minimum and maximum values. A finer-grained alternative is per-channel quantization for weights and per-token quantization for activations, where each input channel of the weights or each token of the activations shares the same quantization parameters. For low-bit quantization scenarios, even finer granularity, per-group quantization, is often employed to further enhance performance. In this case, the elements within a single channel or token are subdivided into groups of a predefined size, with each group quantized independently using its own parameters.

Finer granularity typically leads to improved performance but also incurs higher memory overhead due to the need to store more quantization parameters. Besides, as QServe [17] mentioned, per-group quantization will also raise computational cost in hardware level. Therefore, while finer granularity can enhance accuracy, it may also reduce the overall efficiency of the system. In weight-only quantization, papers such as GPTQ [8], AWQ [11], and QuIP [9] all employ per-group quantization to further enhance performance. For weight-activation quantization, Atom [1] also adopts a per-group quantization strategy. However, with the introduction of rotation-based methods in QuaRot [13] and SpinQuant [3], the performance of per-channel quantization has been significantly improved. Inspired by this, subsequent papers like FlatQuant [12], ResQ [19], and OSTQuant [4] have also adopted per-channel granularity for quantization.

2.5. MXFP4 data format

Recently, the NVIDIA’s GeForce RTX 50 Series based on NVIDIA’s Blackwell architecture [22] is released, which has enabled very low-precision operations using FP4 variants like MXFP4 [23, 24] and NVFP4 [25]. MXFP4 stores each value in an E2M1 format, consisting of one sign bit, one mantissa bit, and two exponent bits. Unlike the INT4 format, MXFP4 employs a fixed granularity, utilizing symmetric per-group quantization with a group size of 32. Each group is associated with an E8M0 scaling factor, and this rescaling process is hardware-integrated.

The value of an encoding MXFP4 data is represented as:

$$\text{value} = \begin{cases} (-1)^S \times 2^{1-\text{bias}} \times (0 + 2^{-m} \times M) & \text{if } E = 0 \\ (-1)^S \times 2^{E-\text{bias}} \times (1 + 2^{-m} \times M) & \text{if } E > 0 \end{cases} \quad (17)$$

where S, E, M corresponds to the sign,exponent and mantissa fields, respectively. The bias is the exponent bias which is set to 1 for MXFP4. So the MXFP4 encoding values are $[-6, -4, -3, -2, -1.5, -1, -0.5, 0, 0.5, 1, 1.5, 2, 3, 4, 6]$.

The quantization process of MXFP4 is similar to the integer quantization process. First, we compute the scaling factor, using the same way as symmetric quantization situation mentioned above that computes from the maximum value of a group of values. Then the scaling factors need to be cast to E8M0 format. After scaling, the values are quantized to the nearest MXFP4 encoding values.

MXFP4 is enable to better handle long-tail distributions compared to INT4, as its values are non-uniformly distributed. In LLMs, both weights and activations approximately follow normal distributions, with activations particularly exhibiting long-tail characteristics. Fig. 5 shows the weight distribution under BF16, INT4, and MXFP4. A clear observation is that under INT4 quantization, values with larger absolute magnitudes represent fewer data points, whereas MXFP4 more fully utilizes the representational capacity of 4-bit precision. Therefore, MXFP4 is more suitable than INT4 as a quantization data type.

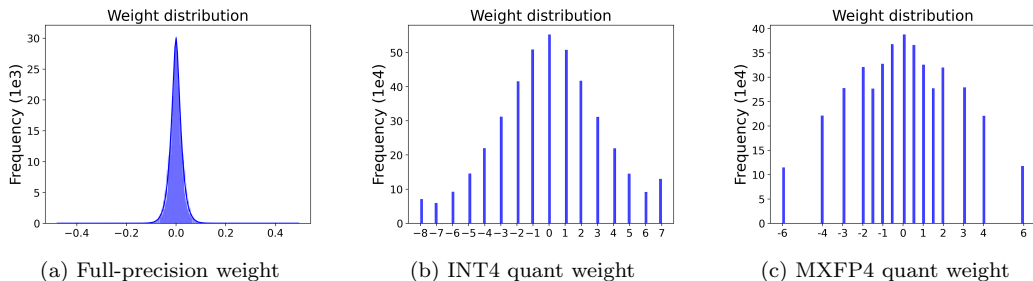


Figure 5: Weight distribution of a q_proj layer of LLaMA-3.2-1B. (a): Weight distribution in full-precision(BF16). (b): Weight distribution after INT4 quantization (group size=32), compared with MXFP4. (c): Weight distribution after MXFP4 quantization.

LLM-FP4 [26] studies FP4 precision quantization for LLMs, including searching for the optimal exponent bias and maximal quantization value. It also proposed a pre-shifted exponent bias technique to address the issue of high inter-channel variance. FP4-Quantization [27] improves the FP4 data representation while introducing a method called LREC (low-rank error calibration) to quantize weights into FP4.

3. Extensive Evaluations

Quantization settings We conduct experiments using W4A4 precision, comparing the results with the origin precision (BF16 or FP16). In the main results, we use per-token or per-group (group size=128) asymmetric quantization for activations. For weight quantization, we use per-channel or per-group (group size=128) symmetric quantization, where we extract the clipping ratio using a linear search over the squared error.

Models and tasks. We conduct experiments on LLaMA-3.2-1B, LLaMA-3.2-3B, and Qwen-2.5-3B. We evaluate their perplexity on the WikiText-2 dataset [28] and assess their accuracy on several zero-shot evaluation tasks, including commonsense reasoning, mathematics, sentiment analysis, and question answering. Specifically, we utilize the following datasets for evaluation: MMLU [29], SST2 [30], MathQA [31], ARC-C [32], HellaSwag [33], Winogrande [34], BoolQ [35], LAMBADA [36], and PIQA [37].

Implementation. To calibrate the GPTQ [8] quantization and the low-rank compensation branch, we use 128 samples from WikiText-2 with a sequence length of 2048. The training of the learnable orthogonal and scaling matrices follows OSTQuant [4] procedure, using 1,000 samples from WikiText-2 and optimized with RiemannAdam. For the low-rank branch, we set the rank $k=32$ and store the low-rank matrices in FP16. For the non-trainable scaling matrix, we follow the SmoothQuant [6] calibration scheme with $\alpha=0.5$.

3.1. Overall performance

Evaluate Methods		Channel		Group-128	
DN	EC	Wiki2-PPL(↓)	0-shot ⁹ Avg.(↑)	Wiki2-PPL(↓)	0-shot ⁹ Avg.(↑)
BF16		9.76	54.78	9.76	54.78
rotation	-	17.83	45.24	14.84	47.51
rotation	low-rank	17.16	45.47	14.5	47.04
rotation	GPTQ	12.95	47.79	11.65	49.38
rotation	GPTQ+low-rank	12.81	48.35	11.61	50.49
rotation+scaling	-	14.88	46.41	13.3	49.22
rotation+scaling	low-rank	14.58	46.76	13.07	49.95
rotation+scaling	GPTQ	11.8	48.89	10.89	50.63
rotation+scaling	GPTQ+low-rank	11.73	49.06	10.87	51.83

Table 3: Evaluation of Quantization Method Combinations, in which rotation or scaling is optimized, in terms of Perplexity on WikiText2 and averaged accuracy on nine Zero-Shot tasks across per-channel and per-group settings of LLaMA-3.2-1B.

Evaluate Methods		Channel		Group-128	
DN	EC	Wiki2-PPL(↓)	0-shot ⁹ Avg.(↑)	Wiki2-PPL(↓)	0-shot ⁹ Avg.(↑)
BF16		9.76	54.78	9.76	54.78
rotation	–	20.31	43.26	15.18	46.62
rotation	low-rank	19.84	43.09	14.83	46.87
rotation	GPTQ	13.31	48.02	11.96	50.05
rotation	GPTQ+low-rank	13.28	48.37	11.98	50.48
rotation+scaling	–	20.96	42.87	16.25	45.01
rotation+scaling	low-rank	21.97	43.07	15.55	45.46
rotation+scaling	GPTQ	14.04	47.53	12.23	48.95
rotation+scaling	GPTQ+low-rank	13.91	46.46	12.17	49.41

Table 4: Evaluation of Quantization Method Combinations, in which rotation or scaling is non-optimized, in terms of Perplexity on WikiText2 and averaged accuracy on nine Zero-Shot tasks across per-channel and per-group settings of LLaMA-3.2-1B.

We select two of the most widely-used pre-quantization transformation techniques, scaling and rotation, and combined them with two quantization error mitigation methods: GPTQ and low-rank branch compensation. A series of experiments are conducted to evaluate these combinations. Table 3 presents the results of using optimized scaling and rotation, illustrating the performance of different method combinations. Table 4 presents the results obtained with randomly initialized rotations and calibrated scaling factors.

Our experiments reveal that the best performance is achieved when both optimized scaling and rotation are applied in conjunction with GPTQ and the low-rank branch. This configuration yields a perplexity of 11.73 in per-channel quantization for Llama-3.2-1B model, which is close to the BF16 baseline of 9.76.

Between the two quantization error mitigation methods, GPTQ clearly plays a more significant role than low-rank adaptation. Under the optimal pre-quantization transformation setting (optimized rotation and scaling), using GPTQ alone results in perplexity of 11.8, whereas using only the low-rank method yields 14.58, under the per-channel settings. When both methods are used together, performance improves further, from 11.8 to 11.73 in the per-channel setting, and from 10.89 to 10.87 in the per-group setting, narrowing the gap to the full-precision model.

In addition, using both optimized rotation and scaling improves performance over using only optimized rotation. However, when employing non-optimized rotation and scaling, rotation alone tends to yield better results than the combination, which indicates that calibrated scaling may not perform well together with rotation in W4A4 settings.

Model	precision	Wiki2 PPL(\downarrow)	Zero-Shot Accuracy(\uparrow)									
			General MMLU	Sentiment SST2	Math MathQA	Reasoning			QA			Avg.
						PiQA	HellaS	WinoG	BoolQ	Lambada	Arc-C	
Llama-3.2-1B	fp16	9.76	36.76	66.86	28.94	74.65	63.67	60.38	63.67	62.1	36.01	54.78
	w4a4	11.73	29.21	55.28	25.43	69.15	57.93	56.43	59.02	56.78	32.34	49.06
Llama-3.2-3B	fp16	7.82	54.06	73.62	34.47	77.48	73.58	69.46	72.97	70.08	46.08	63.53
	w4a4	8.9	46.7	68.58	30.55	73.99	69.54	65.43	68.75	65.32	41.55	58.93
Qwen-2.5-3B	fp16	8.03	65.13	90.37	37.15	78.73	73.55	68.75	77.58	66.8	47.35	67.27
	w4a4	9.22	56.32	69.15	32.5	74.16	67.52	62.12	65.41	57.77	42.83	58.64

Table 5: Comparison of symmetric and asymmetric quantization in Terms of Perplexity on WikiText2 and averaged accuracy on Zero-Shot tasks of LLaMA-3.2-1B

In Table 5, we further conduct experiments on different models: LLaMA-3.2-1B, LLaMA-3.2-3B, and Qwen-2.5-3B, using the optimized scaling and rotation, and combined them with GPTQ and an additional low-rank branch.

3.2. Symmetric vs. asymmetric

Granularity	Metric	rotation+scaling+GPTQ				rotation+scaling+GPTQ+low-rank			
		Sym	W-Asym	A-Asym	Asym	Sym	W-Asym	A-Asym	Asym
channel	Wiki2-PPL(\downarrow)	12.73	12.7	11.8	11.7	12.63	12.65	11.73	11.64
	Arc-Challenge Score(%)	31	31.7	33.3	33.7	31.9	29.9	32.3	32.7

Table 6: Comparison of symmetric and asymmetric quantization in terms of Perplexity on WikiText2 and Arc [32] accuracy of LLaMA-3.2-1B

In Table 6, we evaluate the performance of applying symmetric or asymmetric quantization to weights and activations, respectively. The results demonstrate that asymmetric quantization for activations leads to a significant improvement over symmetric quantization, while the performance gain for weights is relatively minor. We attribute this to the fact that activation distributions tend to be asymmetric, whereas weights are generally more symmetric in distribution.

Therefore, an effective configuration is to use symmetric quantization for weights and asymmetric quantization for activations. This setup not only achieves much better performance than fully symmetric quantization, but also reduces the computational overhead associated with dequantization process, compared to fully asymmetric quantization for both weights and activations.

3.3. Granularity

As illustrated in Fig. 6, we conduct a comprehensive comparison of per-group quantization performance across varying group sizes, measured by perplexity on WikiText2. The experimental results reveal that finer quantization granularity yields superior model performance (lower perplexity), albeit at the expense of elevated storage requirements for quantization parameters. This trade-off stems primarily from the FP16-format scaling factors, whose storage overhead scales inversely with group size. Quantitative analysis of these additional bit costs is presented in Table 7, which compares the average bit overhead introduced by scaling factors under symmetric weight quantization.

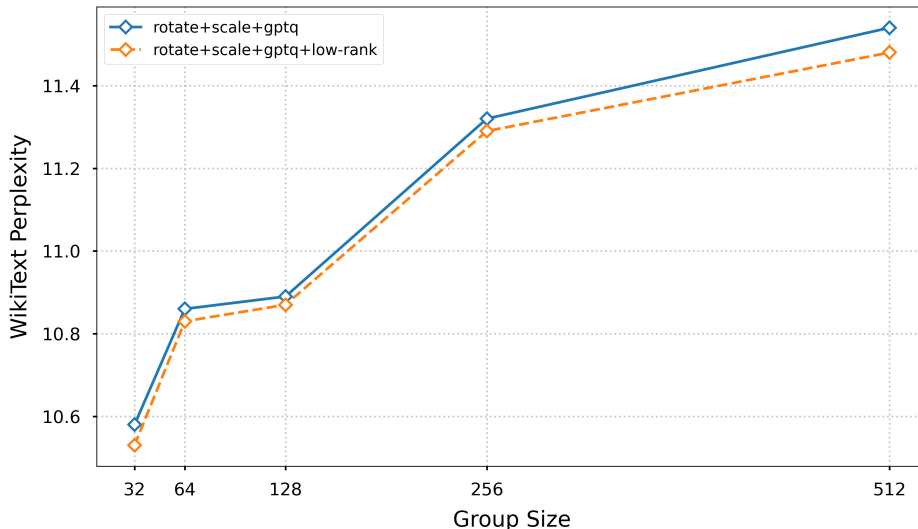


Figure 6: Comparison of different group sizes of quantization in terms of Perplexity on WikiText2 and averaged accuracy on Zero-Shot tasks of LLaMA-3.2-1B

Granularity	group-32	group-64	group-128	group-256	group-512
Average Extra bits	0.5	0.25	0.125	0.0625	0.03125

Table 7: Average extra bits introduced by scaling factors of different granularities

3.4. MXFP4 vs. INT4

Extending experiments to the MXFP4 format, we follow MXFP4 configurations implementing symmetric quantization with group size 32. For acti-

vations, we use a clipping threshold of $3/4$. For weights, we follow the experiments of INT4 quantization, using a linear search over the squared error to find a best clipping ratio. First, we apply no extra pre-quantization transformation or quantization error mitigation process, conducting experiments using only RTN (round to nearest). Table 8 demonstrates that, MXFP4 shows much better performance than INT4 (per-channel).

Error compensation	Data Format		
	INT4 (channel)	INT4 (g-32)	MXFP4
-	923.72	14.19	15.19
GPTQ	1007.33	14.73	13.18
low-rank	723.54	14.04	15.59
GPTQ+low-rank	578.61	12.48	12.72

Table 8: Evaluation of MXFP4 format quantization without using pre-quantization transformation, in terms of Perplexity on WikiText2 of LLaMA-3.2-1B.

Evaluate Methods		WikiText2PPL(↓)	
Data Normalization	Error Compensation	INT4(channel)	MXFP4
scaling	GPTQ	134.85	13.06
scaling	low-rank	165.4	14.83
scaling	GPTQ+low-rank	124.56	12.64
optimized rotation+scaling	GPTQ	11.8	12.61
optimized rotation+scaling	low-rank	14.58	15.53
optimized rotation+scaling	GPTQ+low-rank	11.73	12.29

Table 9: Evaluation of MXFP4 format quantization, in terms of Perplexity on WikiText2 of LLaMA-3.2-1B.

Further, we conduct experiments using both pre-quantization transformation and quantization error mitigation techniques. Results in Table 9 demonstrate that both pre-quantization transformation and quantization error mitigation techniques achieve competitive performance under MXFP4 quantization, confirming the direct applicability of INT4 quantization methods to FP4. Crucially, scaling-based approaches proved more effective than rotation-based methods for MXFP4 — a reversal of their relative efficacy observed in INT4 quantization scenarios.

4. Conclusions

In this paper, we have presented an experimental evaluation of Large language model quantization. We systematically decouple the commonly used quantization methods into two key steps: pre-quantization transformation and quantization error mitigation. After a comprehensive review of existing approaches, we choose scaling and rotation in pre-quantization transformation step, GPTQ and low-rank compensation in quantization error mitigation step to further conduct experimental evaluations on the same ground. We found that uses the optimized rotation and scaling, together with two compensation methods demonstrating the best performance. For quantization settings, asymmetric quantization and smaller group sizes yield better results. For MXFP4 quantization, we can adopt methods used in INT4 quantization. However, using scaling-based pre-quantization transformation demonstrates superior performance compared to INT4. To achieve optimal performance under MXFP4 quantization, further investigation is required to explore its full potential and limitations.

References

- [1] Y. Zhao, C.-Y. Lin, K. Zhu, Z. Ye, L. Chen, S. Zheng, L. Ceze, A. Krishnamurthy, T. Chen, B. Kasikci, Atom: Low-bit quantization for efficient and accurate llm serving, *MLSys* 6 (2024) 196–209.
- [2] W. Shao, M. Chen, Z. Zhang, P. Xu, L. Zhao, Z. Li, K. Zhang, P. Gao, Y. Qiao, P. Luo, Omniquant: Omnidirectionally calibrated quantization for large language models, *arXiv preprint arXiv:2308.13137* (2023).
- [3] Z. Liu, C. Zhao, I. Fedorov, B. Soran, D. Choudhary, R. Krishnamoorthi, V. Chandra, Y. Tian, T. Blankevoort, Spinqant: Llm quantization with learned rotations, *arXiv preprint arXiv:2405.16406* (2024).
- [4] X. Hu, Y. Cheng, D. Yang, Z. Xu, Z. Yuan, J. Yu, C. Xu, Z. Jiang, S. Zhou, Ostquant: Refining large language model quantization with orthogonal and scaling transformations for better distribution fitting, *arXiv preprint arXiv:2501.13987* (2025).
- [5] T. Dettmers, M. Lewis, Y. Belkada, L. Zettlemoyer, Gpt3. int8 (): 8-bit matrix multiplication for transformers at scale, *Advances in neural information processing systems* 35 (2022) 30318–30332.

- [6] G. Xiao, J. Lin, M. Seznec, H. Wu, J. Demouth, S. Han, Smoothquant: Accurate and efficient post-training quantization for large language models, in: ICML, PMLR, 2023, pp. 38087–38099.
- [7] X. Wei, Y. Zhang, Y. Li, X. Zhang, R. Gong, J. Guo, X. Liu, Outlier suppression+: Accurate quantization of large language models by equivalent and optimal shifting and scaling, arXiv preprint arXiv:2304.09145 (2023).
- [8] E. Frantar, S. Ashkboos, T. Hoefler, D. Alistarh, Gptq: Accurate post-training quantization for generative pre-trained transformers, arXiv preprint arXiv:2210.17323 (2022).
- [9] J. Chee, Y. Cai, V. Kuleshov, C. M. De Sa, Quip: 2-bit quantization of large language models with guarantees, NeurIPS 36 (2023) 4396–4429.
- [10] A. Tseng, J. Chee, Q. Sun, V. Kuleshov, C. De Sa, Quip#: Even better llm quantization with hadamard incoherence and lattice codebooks, arXiv preprint arXiv:2402.04396 (2024).
- [11] J. Lin, J. Tang, H. Tang, S. Yang, W.-M. Chen, W.-C. Wang, G. Xiao, X. Dang, C. Gan, S. Han, Awq: Activation-aware weight quantization for on-device llm compression and acceleration, MLSys 6 (2024) 87–100.
- [12] Y. Sun, R. Liu, H. Bai, H. Bao, K. Zhao, Y. Li, J. Hu, X. Yu, L. Hou, C. Yuan, et al., Flatquant: Flatness matters for llm quantization, arXiv preprint arXiv:2410.09426 (2024).
- [13] S. Ashkboos, A. Mohtashami, M. L. Croci, B. Li, P. Cameron, M. Jaggi, D. Alistarh, T. Hoefler, J. Hensman, Quarot: Outlier-free 4-bit inference in rotated llms, NeurIPS 37 (2024) 100213–100240.
- [14] Z. Yao, X. Wu, C. Li, S. Youn, Y. He, Zeroquant-v2: Exploring post-training quantization in llms from comprehensive study to low rank compensation, arXiv preprint arXiv:2303.08302 (2023).
- [15] C. Zhang, J. T. Wong, C. Xiao, G. A. Constantinides, Y. Zhao, Qera: an analytical framework for quantization error reconstruction, arXiv preprint arXiv:2410.06040 (2024).

- [16] R. Saha, N. Sagan, V. Srivastava, A. Goldsmith, M. Pilanci, Compressing large language models using low rank and low precision decomposition, *NeurIPS* 37 (2024) 88981–89018.
- [17] Y. Lin, H. Tang, S. Yang, Z. Zhang, G. Xiao, C. Gan, S. Han, Qserve: W4a8kv4 quantization and system co-design for efficient llm serving, *arXiv preprint arXiv:2405.04532* (2024).
- [18] C. Zhang, J. Cheng, G. A. Constantinides, Y. Zhao, Lqer: Low-rank quantization error reconstruction for llms, *arXiv preprint arXiv:2402.02446* (2024).
- [19] U. Saxena, S. Sharify, K. Roy, X. Wang, Resq: Mixed-precision quantization of large language models with low-rank residuals, *arXiv preprint arXiv:2412.14363* (2024).
- [20] E. Frantar, D. Alistarh, Optimal brain compression: A framework for accurate post-training quantization and pruning, *NeurIPS* 35 (2022) 4475–4488.
- [21] M. Fu, H. Yu, J. Shao, J. Zhou, K. Zhu, J. Wu, Quantization without tears, in: *CVPR*, 2025, pp. 4462–4472.
- [22] NVIDIA Corporation, *NVIDIA Blackwell GPU Architecture* (2024).
- [23] B. D. Rouhani, R. Zhao, A. More, M. Hall, A. Khodamoradi, S. Deng, D. Choudhary, M. Cornea, E. Dellinger, K. Denolf, et al., Microscaling data formats for deep learning, *arXiv preprint arXiv:2310.10537* (2023).
- [24] Open Compute Project, *OCP Microscaling Formats (MX) Specification* (2024).
- [25] N. Corporation, *BlockScaling: NVFP4 Datatype*. (2021).
- [26] S.-y. Liu, Z. Liu, X. Huang, P. Dong, K.-T. Cheng, Llm-fp4: 4-bit floating-point quantized transformers, *arXiv preprint arXiv:2310.16836* (2023).
- [27] J. Wang, H. Liu, D. Feng, J. Ding, B. Ding, Fp4-quantization: Lossless 4bit quantization for large language models, in: *JCC, IEEE*, 2024, pp. 61–67.

- [28] S. Merity, C. Xiong, J. Bradbury, R. Socher, Pointer sentinel mixture models (2016). arXiv:1609.07843.
- [29] D. Hendrycks, C. Burns, S. Basart, A. Zou, M. Mazeika, D. Song, J. Steinhardt, Measuring massive multitask language understanding, ICLR (2021).
- [30] R. Socher, A. Perelygin, J. Wu, J. Chuang, C. D. Manning, A. Ng, C. Potts, Recursive deep models for semantic compositionality over a sentiment treebank, in: EMNLP, Association for Computational Linguistics, Seattle, Washington, USA, 2013, pp. 1631–1642.
- [31] A. Amini, S. Gabriel, P. Lin, R. Koncel-Kedziorski, Y. Choi, H. Hajishirzi, Mathqa: Towards interpretable math word problem solving with operation-based formalisms, arXiv preprint arXiv:1905.13319 (2019).
- [32] M. Boratko, H. Padigela, D. Mikkilineni, P. Yuvraj, R. Das, A. McCallum, M. Chang, A. Fokoue-Nkoutche, P. Kapanipathi, N. Mattei, et al., A systematic classification of knowledge, reasoning, and context within the arc dataset, arXiv preprint arXiv:1806.00358 (2018).
- [33] R. Zellers, A. Holtzman, Y. Bisk, A. Farhadi, Y. Choi, Hellaswag: Can a machine really finish your sentence?, arXiv preprint arXiv:1905.07830 (2019).
- [34] K. Sakaguchi, R. L. Bras, C. Bhagavatula, Y. Choi, Winogrande: An adversarial winograd schema challenge at scale, arXiv preprint arXiv:1907.10641 (2019).
- [35] C. Clark, K. Lee, M.-W. Chang, T. Kwiatkowski, M. Collins, K. Toutanova, Boolq: Exploring the surprising difficulty of natural yes/no questions, arXiv preprint arXiv:1905.10044 (2019).
- [36] A. Radford, J. Wu, R. Child, D. Luan, D. Amodei, I. Sutskever, et al., Language models are unsupervised multitask learners, OpenAI blog 1 (8) (2019) 9.
- [37] Y. Bisk, R. Zellers, J. Gao, Y. Choi, et al., Piqa: Reasoning about physical commonsense in natural language, in: AACL, 2020, pp. 7432–7439, vol. 34, No. 5.